PHYSICAL REVIEW B VOLUME 48, NUMBER 4 15 JULY 1993-II

Elastic lattice deformation of semiconductor heterostructures grown on arbitrarily oriented substrate surfaces

Liberato De Caro and Leander Tapfer

Centro Nazionale Ricerca e Sviluppo Materiali, S.S. 7 per Mesagne km 7,300, I-72100 Brindisi, Italy

(Received 21 September 1992; revised manuscript received 2 February 1993)

We present a theoretical study of the lattice deformation of semiconductor epitaxial layers grown on arbitrarily oriented substrates, both with cubic symmetry. We assume a coherent (pseudomorphic) interface between the epitaxial layer and the substrate, i.e., without defects and dislocations. The elastic strain tensor components are calculated by minimization of the strain-energy density. A detailed study of the tetragonal deformation and of the shear strain is presented. We obtained no shear strain for the high-symmetry surfaces [001], [110], and [111], while for all the other surface orientations, which do not even have twofold symmetry, a shear strain was obtained with the highest value for the [113] surface. The shear strain has the opposite sign for $[kk1]$ surfaces with respect to $[11k]$ surfaces. In addition, the shear displacement occurs in all cases normal to the direction of highest symmetry of the interface plane.

I. INTRODUCTION

Most studies of semiconductor heterostructures are reported on materials grown on (001)-oriented substrates and other high-symmetry surfaces, i.e., [110] and [111] surfaces. However, recently there has been an increasing interest in the physical properties of semiconductor heterostructures grown pseudomorphically on low-symmetry surfaces. The growth, the optical and electronic properties of semiconductor heterostructures were investigated theoretically and experimentally and are reported for (211),[1-3] (311),[3-9] (511),[10,11] (221),[2] (331),[12] (210),[13] and (310) (Ref. 14) substrate surfaces. These studies show that the surface reconstruction during the growth, the surface morphology, the lattice deformation, the incorporation of impurity atoms (dopants), the bond configuration, and the sticking coefficient of atoms change drastically with the surface orientation. The growth on corrugated or patterned surfaces occurs on submicrometer facets, which are high-index surfaces with low crystallographic symmetry.[3,9,15-17]

The lattice deformation and the strain fields generate electric fields in epitaxial layers and affect the microscopic properties, i.e., the degeneracy of the valence band and change of the band gap,[18,19] as well as macroscopic properties, i.e., piezoelectric and photoelastic effects of crystals.[20] This is of great importance for the design and development of new optoelectronic and electronic devices. Therefore, in order to optimize the growth and to understand the physical properties of epitaxial layers, it is of fundamental importance to specify and characterize the lattice deformation and strain fields of the crystal unit cell. Usually, the strain fields in epitaxial layers can be measured with high accuracy by high-resolution x-ray-diffraction experiments.[21] However, a correct interpretation of the x-ray-diffraction data requires an accurate knowledge of the geometrical deformation of the unit cells of the material system under consideration.

The state of strain in epitaxial layers can be determined by solving the equations of the elasticity theory using Hooke's law and appropriate boundary conditions.[22,23] Very recently, Caridi and Stark calculated the strain tensor elements of strained $[hhk]$-oriented cubic crystals by minimizing the strain-energy density via the commensurability constraint.[24] However, imposing this constraint, only the symmetrical part of the strain tensor was considered. In this case, even for low-symmetry surfaces, no shear strain was obtained.

In this paper, we investigate the lattice deformation due to elastic strain caused by the lattice mismatch between epitaxial film and substrate, i.e., only pseudomorphic semiconductor heterostructures with a coherent interface are studied. We assume that the growth mode of the epitaxial films is the layer-by-layer growth (Frank–van der Merwe) and no islanding and lattice relaxation (generation of misfit dislocations) occur.[25,26] We obtain the general expressions for the unit-cell deformation, tetragonal distortion, and shear strain of epitaxial layers with cubic symmetry by minimizing the strain energy starting from the commensurability constraint (coherent interface) and using all the asymmetric elastic strain tensor. We show that the shear strain is different from zero for all surface directions, except for the high-symmetry [001], [110], and [111] surfaces.

II. COMMENSURABILITY CONSTRAINT AND STRAIN-ENERGY DENSITY

Let us consider a crystalline epitaxial layer deposited onto a substrate crystal, both with cubic symmetry. For cubic materials the lattice translation vectors $\mathbf{f}_i^L$ and $\mathbf{f}_i^S$ of the layer and the substrate are in the strain-free state, given by

$$\mathbf{f}_i^L = d_L \mathbf{x}_i \qquad \mathbf{f}_i^S = d_S \mathbf{x}_i \, , \tag{1}$$

 ©1993 The American Physical Society

where $i=\{1,2,3\}$ and d_L and d_S are the lattice constants of the layer (L) and substrate (S), respectively.

If the crystal is deformed, the distorted lattice translation vectors can be written in terms of the crystalline unit vectors. By definition of the strain tensor, we have

$$\mathbf{F}_i^{\alpha}=d_\alpha(\delta_{ij}+A_{ij})\mathbf{x}_j \ , \tag{2}$$

where $i,j=\{1,2,3\}$, $\alpha=\{L,S\}$, δ_{ij} is the Kronecker δ tensor and A_{ij} is the elastic strain tensor. If we consider a crystalline elastic medium with cubic symmetry, which obeys Hooke's law and is defect free, the total strain tensor S_{ij} is given by[27]

$$S_{ij}=A_{ij}+B_{ij}=A_{ij}+\varepsilon^{\parallel}\delta_{ij} \ , \tag{3}$$

where B_{ij} is the misfit of the lattice-parameter tensor and $\varepsilon^{\parallel}=(d_S-d_L)/d_L$. Here we are using the continuum elasticity theory and the bulk elastic stiffness constants. This assumption is valid since a breakdown of the continuum elasticity theory was observed only for monoatomic films.[28]

The work per unit volume which is necessary to produce an elastic strain ε_{ij} is called the strain-energy density, and for a cubic crystal is given by

$$\begin{aligned} U=C_{11}(\varepsilon_{11}^2+\varepsilon_{22}^2+\varepsilon_{33}^2) \\ +C_{12}(\varepsilon_{22}\varepsilon_{33}+\varepsilon_{33}\varepsilon_{11}+\varepsilon_{11}\varepsilon_{22}) \\ +2C_{44}(\varepsilon_{12}^2+\varepsilon_{23}^2+\varepsilon_{13}^2) \ , \end{aligned} \tag{4}$$

where C_{11}, C_{12}, and C_{44} are the three elastic stiffness tensor elements, which for a cubic lattice are independent, and ε_{ij} is the symmetrical part of the elastic strain tensor:

$$\varepsilon_{ij}=\tfrac{1}{2}(A_{ij}+A_{ji}) \ . \tag{5}$$

The antisymmetrical part gives the rotation of the strained crystal and therefore does not make any contribution to the work done.[29]

The elastic strain tensor components of the layer and substrate, after the deformation, can be calculated by imposing the equilibrium condition via the minimization of the strain-energy density. First we consider two lattice-mismatched epitaxial layers with the lattice constants d_S and d_L, respectively. If no plastic deformation occurs (generation of misfit dislocations) at the heterointerface even after the deformation (coherent or pseudomorphic growth), the lattice translation vectors of each strained material must have a common projection onto the growth plane. These boundary conditions are known as the lattice commensurability constraint:

$$\begin{aligned} \mathbf{F}_i^L\cdot\mathbf{x}_1'=\mathbf{F}_i^S\cdot\mathbf{x}_1' \ , \\ \mathbf{F}_i^L\cdot\mathbf{x}_2'=\mathbf{F}_i^S\cdot\mathbf{x}_2' \ , \end{aligned} \tag{6}$$

where $\mathbf{x}_1'$ and $\mathbf{x}_2'$ are two orthogonal unit vectors in the interface plane (Fig. 1), with $i=\{1,2,3\}$. It should be noted that the constraint given by Eq. (6) is valid for the epitaxial layer with the same azimuthal orientation of the substrate crystal. Therefore, mixed orientations which may occur in highly mismatched material system are not considered by these constraint conditions.[30] Moreover,

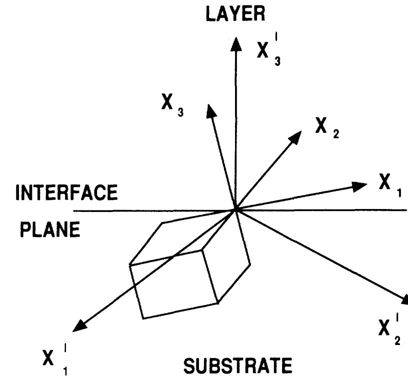

FIG. 1. The schematic diagram of a unit cell with cubic symmetry deposited onto a substrate crystal of arbitrary surface orientation. The crystallographic reference system $\{\mathbf{x}_i\}$ and the "epitaxial-film" one $\{\mathbf{x}_i'\}$ are shown. The axis $\mathbf{x}_3'$ is normal to the interface.

we assume that the epitaxial layer is much thinner than the substrate and, therefore, all the strain occurs in the overlayer:

$$\mathbf{F}_i^S=\mathbf{f}_i^S \ , \tag{7}$$

with $i=\{1,2,3\}$.

From Eqs. (1), (2), (3), and (7), it follows that the commensurability constraint can be written as

$$\mathbf{S}_{ij}\mathbf{f}_j\cdot\mathbf{x}_1'=0 \ , \tag{8a}$$

$$\mathbf{S}_{ij}\mathbf{f}_j\cdot\mathbf{x}_2'=0 \ . \tag{8b}$$

Due to the strain, along the arbitrary direction $\mathbf{P}$, the displacement is given by $D_i=S_{ij}P_j$, where the P_j's are the components of the vector $\mathbf{P}$ with respect to the crystallographic axes $\mathbf{x}_j$. It is easy to verify from Eqs. (8) that the commensurability constraint is equivalent to the condition of making the in-plane displacements equal to 0 for all directions in the interface plane (Fig. 2), i.e., the so-called pseudomorphic growth of the strained layer which does not lead to the formation of misfit dislocations [Fig. 2(c)]. Moreover, in order to determine the symmetry of the deformation, it is useful to calculate the strain tensor elements with reference to the coordinate system $\mathbf{x}_1'$, $\mathbf{x}_2'$, and $\mathbf{x}_3'$ of the epitaxial film, where $\mathbf{x}_3'$ is the axis normal to the interface. Using this new reference system, the commensurability constraint implies

$$S_{ij}'P_j'=0 \ , \tag{9}$$

where

$$\begin{aligned} S_{ij}'=T_{ik}T_{j1}S_{k1} \ , \\ P_j'=T_{jk}P_k \ . \end{aligned} \tag{10}$$

T_{ik} is the matrix of the transformation from the crystallographic reference system to the epitaxial layer reference system, and is given by

$$T_{ik}=\mathbf{x}_i'\cdot\mathbf{x}_k \ . \tag{11}$$

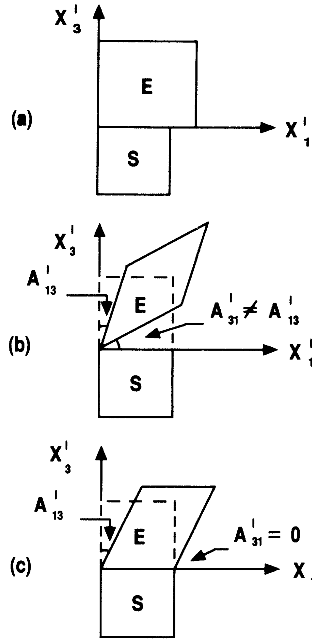

FIG. 2. The schematic diagram of the unit cells of the epitaxial layer (E) and the substrate crystal (S) in the $(\mathbf{x}'_1,\mathbf{x}'_3)$ plane. (a) Without lattice deformation of the unit cell of the epitaxial layer (E). (b) Lattice deformation of the unit cell E considering shear strain as well as lattice rotation, with respect to the substrate unit cell showing the incoherence between epitaxial layer and substrate. (c) Lattice deformation and shear strain of the epitaxial layer (E) with respect to the substrate unit cell in the case of a coherent interface (pseudomorphic growth).

For $\mathbf{P}=\mathbf{x}'_1$ and $\mathbf{x}'_2$ [see Fig. 2(c)], Eq. (9) gives

$$S'_{i1}=0 \, , \quad S'_{i2}=0 \, , \tag{12}$$

respectively. Substituting Eqs. (12) and (3) into Eq. (5), we obtain

$$\varepsilon'_{11}=\varepsilon^{\parallel} \, , \; \varepsilon'_{22}=\varepsilon^{\parallel} \, , \; \varepsilon'_{33}=S'_{33}+\varepsilon^{\parallel} \, , \quad \varepsilon'_{12}=0 \, , \; \varepsilon'_{13}=S'_{13}/2 \, , \; \varepsilon'_{23}=S'_{23}/2 \, . \tag{13}$$

Thus, from the commensurability constraint, we obtain that the elastic strain in the plane of the interface is isotropic.

III. MINIMIZATION OF THE STRAIN-ENERGY DENSITY

The strain-energy density U can be expressed as a function of ε'_{ij}, and its minimization an be obtained by solving the following system of equations:

$$\frac{\partial U}{\partial \varepsilon'_{13}}(\varepsilon'_{13},\varepsilon'_{23},\varepsilon'_{33})=0 \, , \quad \frac{\partial U}{\partial \varepsilon'_{23}}(\varepsilon'_{13},\varepsilon'_{23},\varepsilon'_{33})=0 \, , \quad \frac{\partial U}{\partial \varepsilon'_{33}}(\varepsilon'_{13},\varepsilon'_{23},\varepsilon'_{33})=0 \, . \tag{14}$$

By definition we have

$$\frac{\partial U}{\partial \varepsilon'_{ij}}=\sigma'_{ij} \, , \tag{15}$$

where σ'_{ij} are the stress tensor elements, with respect to the epitaxial-film reference system.[29] Thus, from Eqs. (14) and (15), it follows that

$$\sigma'_{i3}=0 \, , \tag{16}$$

with $i=\{1,2,3\}$. But the forces which act on the surface are expressed by

$$\mathbf{f}'_i=\sigma'_{ij}(\mathbf{x}'_3)_j=\sigma'_{i3} \, ,$$

which are zero due to Eq. (16). Therefore, the solution which minimizes the strain-energy density leads in the final state to a stress-free surface.[22,23] The explicit expressions of Eqs. (14) are given by

$$(CR_{33}+C_{11}-C)(\varepsilon^{\parallel}-\varepsilon'_{33})-2CR_{34}\varepsilon'_{23}-2CR_{35}\varepsilon'_{13} =(C_{11}+2C_{12})\varepsilon^{\parallel} \, ,$$

$$CR_{34}(\varepsilon^{\parallel}-\varepsilon'_{33})-2(CR_{23}+C_{44})\varepsilon'_{23}-2CR_{36}\varepsilon'_{13}=0 \, , \tag{17}$$

$$CR_{35}(\varepsilon^{\parallel}-\varepsilon'_{33})-2CR_{36}\varepsilon'_{23}-(CR_{13}+C_{44})\varepsilon'_{13}=0 \, ,$$

where $C=C_{11}-C_{12}-2C_{44}$ and

$$R_{\alpha\beta}=T_{i1}T_{j1}T_{k1}T_{l1}+T_{i2}T_{j2}T_{k2}T_{l2}+T_{i3}T_{j3}T_{k3}T_{l3} \, . \tag{18}$$

Here, α and $\beta=\{1,\ldots,6\}$ indicate the symmetric pairs of the indices ij and $kl=\{1,2,3\}$, respectively.[29] The coefficients $R_{\alpha\beta}$ describe the transformation of the stiffness tensor elements from the crystallographic reference system to the epitaxial layer reference system. The solution of Eqs. (17) is the minimum point for the strain-energy density. The results are given by

$$\Delta\varepsilon=\frac{(C_{11}+2C_{12})}{\Delta}\varepsilon^{\parallel}[C_{44}^2+CC_{44}(1-R_{33}) +3C^2(T_{31}T_{32}T_{33})^2] \, ,$$

$$\varepsilon'_{23}=\frac{(C_{11}+2C_{12})}{2\Delta}C\varepsilon^{\parallel}[C_{44}R_{34} +C(R_{31}R_{34}-R_{35}R_{36})] \, , \tag{19}$$

$$\varepsilon'_{13}=\frac{(C_{11}+2C_{12})}{2\Delta}C\varepsilon^{\parallel}[C_{44}R_{35} +C(R_{32}R_{35}-R_{34}R_{36})] \, ,$$

where $\Delta\varepsilon=\varepsilon^{\parallel}-\varepsilon^{\perp}=\varepsilon^{\parallel}-\varepsilon'_{33}$ is the tetragonal distortion, ε'_{13} and ε'_{23} are the shear strain elements, and Δ is given by

$$\Delta=C_{11}C_{44}^2+(CC_{44}/2)(C_{11}+C_{12})(1-R_{33}) +C^2(C_{11}+2C_{12}+C_{44})(T_{31}T_{32}T_{33})^2 \, . \tag{20}$$

IV. CALCULATION OF THE PRINCIPAL STRAINS

The principal strains can be easily obtained solving the characteristic equation

$$|\varepsilon'_{ij}-\lambda\delta'_{ij}|=0 . \tag{21}$$

The eigenvalues are given by the roots

$$\lambda_1=\varepsilon^{\parallel} ,$$
$$\lambda_{2/3}=\tfrac{1}{2}\{\varepsilon^{\parallel}+\varepsilon^{\perp}\pm[(\Delta\varepsilon)^2+4(\varepsilon_s)^2]^{1/2}\} , \tag{22}$$

with

$$\varepsilon_s=[(\varepsilon'_{13})^2+(\varepsilon'_{23})^2]^{1/2} .$$

The symmetrical strain tensor, with respect to the principal axes, is thus

$$\varepsilon''_{ij}=\lambda_i\delta_{ij} , \tag{23}$$

and the principal axes, which represent three mutually perpendicular directions in the crystal, remaining mutually perpendicular during the deformation,[29] are given by

$$\begin{aligned}\mathbf{x}''_1&=(-\varepsilon'_{23}/\varepsilon_s,\varepsilon'_{13}/\varepsilon_s,0) ,\\ \mathbf{x}''_2&=1/[(\varepsilon_s)^2+(\varepsilon^{\parallel}-\lambda_2)^2]^{1/2}[\varepsilon'_{13},\varepsilon'_{23},-(\varepsilon^{\parallel}-\lambda_2)] ,\\ \mathbf{x}''_3&=1/\{\varepsilon_s[(\varepsilon_s)^2+(\varepsilon^{\parallel}-\lambda_2)^2]^{1/2}\}\\ &\quad\times[-\varepsilon'_{13}(\varepsilon^{\parallel}-\lambda_2),-\varepsilon'_{23}(\varepsilon^{\parallel}-\lambda_2),-(\varepsilon_s)^2] .\end{aligned} \tag{24}$$

It is obvious that one of the principal axes ($\mathbf{x}''_1$) always belongs to the interface plane, and it can be chosen as a reference axis in the $\{\mathbf{x}'_i\}$ reference system. Moreover, in the case of a high-symmetry substrate where no shear strain occurs, i.e., $\varepsilon'_{13}=\varepsilon'_{23}=0$, the principal strains become $\lambda_1=\lambda_2=\varepsilon^{\parallel}$ and $\lambda_3=\varepsilon^{\perp}$.

V. TETRAGONAL DEFORMATION AND SHEAR STRAIN ANALYSIS

It can be easily demonstrated that the shear strain elements in Eq. (23) are zero for epitaxial layers grown onto (100), (110), and (111) surfaces, i.e., surfaces with at least twofold symmetry. Thus for these high-symmetry surfaces the only parameter that characterizes the deformation is $\Delta\varepsilon$, and the unit cells are tetragonally distorted. This is true for all material systems with cubic symmetry, and is independent of the magnitude of the lattice mismatch between the epitaxial layer and the substrate crystal. However, for surfaces with lower symmetry, the shear strain elements are in general different from zero. In this case the crystal is rhombohedrically distorted and the magnitude of the deformation is given by $\varepsilon_s/\varepsilon^{\parallel}$. The sign of the shear strain gives the opposite of the shear displacement and depends on the sign of $\varepsilon^{\parallel}$. The unit cell of the epitaxial layer, indicated by the dotted lines parallel to the crystallographic axes $\mathbf{x}_i$ and $\mathbf{x}_j$, with $i\neq j$, is shown schematically in Fig. 2. After the deformation, the edges of the unit cell form an angle of $\pi/2-2\varepsilon'_{ij}$, and the deformation occurs in a plane orthogonal to $\mathbf{x}'_k$, with $k\neq i,j$. In particular, from Eqs. (19) it follows that a sufficient condition for having no shear strains is $R_{35}=R_{34}=0$. However, as shown in Sec. IV, axes $\mathbf{x}'_1$ and $\mathbf{x}'_2$ can always be chosen so that only one of the shear strain components obtained is different from zero. In this way, one of the two axes of the symmetric tensor ε'_{ij} is a principal one ($\mathbf{x}''_1$).

In Fig. 3, we show the tetragonal deformation, normalized to $\varepsilon^{\parallel}$, as a function of the direction cosine T_{33} for

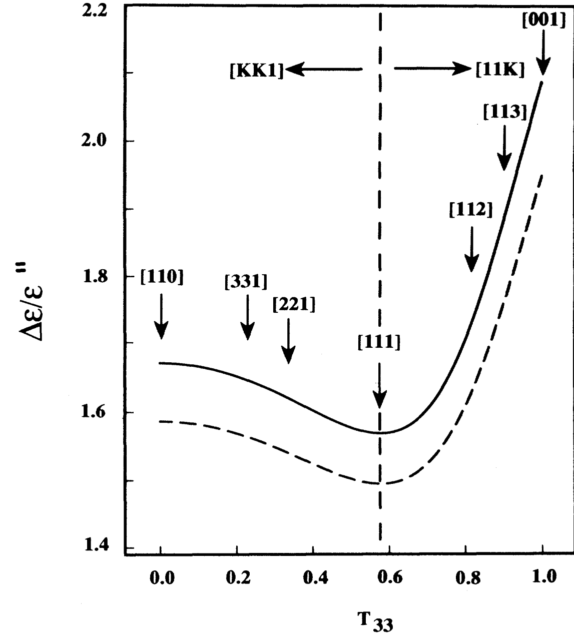

FIG. 3. The normalized tetragonal strain as a function of the direction cosine of the substrate surface.

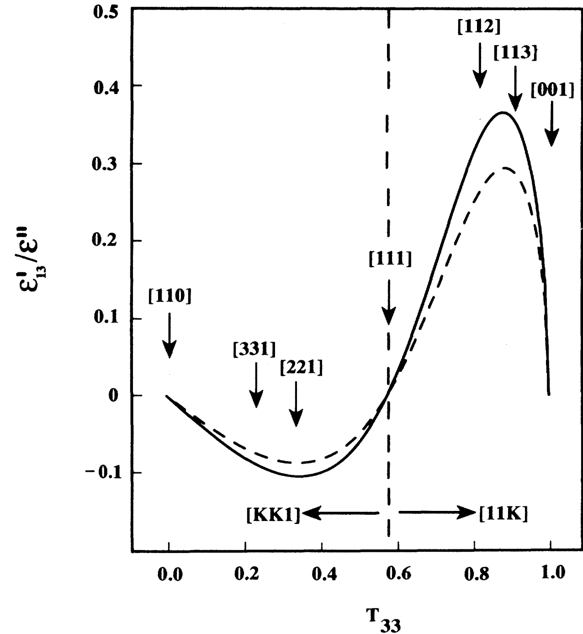

FIG. 4. The normalized shear strain as a function of the direction cosine of the substrate surface.

TABLE I. Tetragonal deformation, shear strain, and shear displacement direction of AlAs and InAs epitaxial layers grown on GaAs substrates of different surface orientations.

Substrate orientation	x_1'	x_2'	$\varepsilon^{\parallel}$ ($\times 10^{-4}$) AlAs	$\varepsilon^{\parallel}$ ($\times 10^{-4}$) InAs	ε_{13}' ($\times 10^{-4}$) AlAs	ε_{13}' ($\times 10^{-4}$) InAs	ε_{23}' ($\times 10^{-4}$) AlAs	ε_{23}' ($\times 10^{-4}$) InAs
100			−13.7	−669	0	0	0	0
110			−13.7	−669	0	0	0	0
111			−13.7	−669	0	0	0	0
120	001	$\bar{2}10$	−13.7	−669	0	0	−3.80	−228
130	001	$3\bar{1}0$	−13.7	−669	0	0	−2.54	−153
112	$11\bar{1}$	$\bar{1}10$	−13.7	−669	−3.65	−218	0	0
113	$33\bar{2}$	$\bar{1}10$	−13.7	−669	−3.97	−240	0	0
114	$22\bar{1}$	$\bar{1}10$	−13.7	-669	−3.45	−205	0	0
115	$55\bar{2}$	$\bar{1}10$	−13.7	−669	−3.06	−182	0	0
221	$11\bar{4}$	$\bar{1}10$	−13.7	−669	1.19	70	0	0
331	$11\bar{6}$	$\bar{1}10$	−13.7	−669	1.04	57	0	0

AlAs (dotted line) and InAs layers (solid line) grown epitaxially on GaAs substrates with orientations $[11k]$ and $[kk1]$, where k is an integer. The exact formula of the tetragonal deformation for the above crystallographic orientation is given in the Appendix [Eqs. (A4)]. It should be noted that the lowest tetragonal deformation is observed for layers grown along the [111] direction, while the highest deformation occurs along the [001] direction (Fig. 3). Moreover, the tetragonal deformation is slowly varying for $[kk1]$ substrate orientations; on the contrary, the tetragonal deformation varies much more for $[11k]$ surfaces. Figure 4 shows the normalized shear strain ($\varepsilon_{13}'/\varepsilon^{\parallel}$) as a function of the direction cosine of the substrate orientation. The exact formula for the shear strain of the above orientations is given in the Appendix [Eqs. (A4)]. The maximum shear strain value is obtained for the [113] substrate orientation. This result is related to the fact that the [113] direction is the orientation with the highest distance from the high-symmetry orientations. Furthermore, the shear strain has an opposite sign for the $[kk1]$ substrate orientations with respect to the $[11k]$ orientations.

In Table I, we report the shear strain values and the shear displacement directions for AlAs and InAs layers grown epitaxially on GaAs substrates for different crystallographic orientations of interest. The shear strain for a certain surface orientation is higher for InAs than for AlAs due to the much higher lattice mismatch between InAs and GaAs ($\approx 7\%$) with respect to the 0.14% lattice mismatch between AlAs and GaAs. It is worth noting that the values of the shear strain are not negligible compared to the hydrostatic component $\varepsilon^{\parallel}$, e.g., $\frac{1}{3}$ of $\varepsilon^{\parallel}$ for the [113] orientation. In addition, the shear displacements always occur in the plane perpendicular to the direction of highest symmetry for the interface plane. This finding is of particular importance for the epitaxial growth on patterned or intentionally corrugated surfaces. The epitaxial growth on corrugated surfaces means that the growth occurs on facets with different orientation.[9,16,17] As we have shown, the deformation of the unit cell strongly depends on the surface orientation, and consequently a "misfit" at the boundary between two growth regions could be obtained, which may generate dislocations and defects. However, it should be noted that the "misfit" between these two growth regions is not generated by a lattice mismatch, but by a different shear displacement of the unit cells.

VI. CONCLUSIONS

In this work, we studied theoretically the strain fields and the lattice deformation of epitaxial layers grown pseudomorphically on arbitrarily oriented substrates using the asymmetric elastic strain tensor and minimizing the strain-energy density. The constituent material of the epitaxial layer and of the substrates has cubic symmetry. We showed that the elasticity theory and the appropriate boundary conditions (commensurability constraints) lead to the presence of shear strains for lower-symmetry surfaces (less than twofold), in contrast to the study reported by Caridi and Stark.[24] For (100), (110), and (111), no shear strain was obtained, in agreement with earlier theoretical and experimental studies.[22,24] We found that the highest shear strain occurs for the [113] surface, while the highest tetragonal deformation occurs along the [001] surface direction. These findings are independent of the epitaxial layer/substrate material system.

APPENDIX

Now we calculate the analytical expressions of the shear strain and the tetragonal deformation as a function of the direction cosine T_{33} for the substrate orientations $[11k]$ and $[kk1]$, where k is an integer. For the $[11k]$ orientations, the relation between T_{33} and k is given by

$$T_{33}=k/(\sqrt{2+k^2}) \quad \text{with} \quad \frac{1}{\sqrt{3}} \le T_{33} \le 1 , \tag{A1}$$

whereas for the $[kk1]$ orientations we have

$$T_{33}=1/(\sqrt{1+2k^2}) \quad \text{with} \quad 0 \le T_{33} \le \frac{1}{\sqrt{3}} . \tag{A2}$$

The axes of the coordinate system are chosen as

$$\mathbf{x}_1' = \frac{1}{\sqrt{2}}(\sqrt{1-T_{33}^2}, \sqrt{1-T_{33}^2}, \sqrt{2}T_{33}) ,$$
$$\mathbf{x}_2' = \frac{1}{\sqrt{2}}(\bar{1},1,0) , \qquad (A3)$$
$$\mathbf{x}_3' = \frac{1}{\sqrt{2}}(T_{33}, T_{33}, -\sqrt{2}\sqrt{1-T_{33}^2}) ,$$

From Eqs. (19) and (20) we obtain, for the tetragonal deformation and the shear strains, the following expressions:

$$\Delta\varepsilon/\varepsilon^{\parallel} = \{(C_{11}+2C_{12})[C_{44}^2+(CC_{44}/2)(1-3T_{33}^4+2T_{33}^2)+(3C^2/4)(T_{33}^2-2T_{33}^4+T_{33}^6)]\}/\Delta ,$$
$$\varepsilon_{23}' = 0 , \qquad (A4)$$
$$\varepsilon_{13}'/\varepsilon^{\parallel} = \frac{(C_{11}+2C_{12})}{2\Delta} C(\sqrt{1-T_{33}^2}\,T_{33})[(C_{44}/2)(1-3T_{33}^2)+(C/4)(1-3T_{33}^4+2T_{33}^2)] ,$$

where

$$\Delta = \{C_{11}C_{44}^2+(CC_{44}/4)(C_{11}+C_{12})(1-3T_{33}^4+2T_{33}^2)+(C^2/4)(C_{11}+2C_{12}+C_{44})(T_{33}^2-2T_{33}^4+T_{33}^6)\} .$$

[1]S. Subbanna, H. Krömer, and J. L. Merz, J. Appl. Phys. **59**, 488 (1986).

[2]P. N. Uppal, J. S. Ahearn, S. P. Svensson, and R. Herring, J. Cryst. Growth **95**, 281 (1989).

[3]R. Nötzel, N. N. Ledentsov, L. Däweritz, M. Hohenstein, and K. Ploog, Phys. Rev. Lett. **67**, 3814 (1991).

[4]W. I. Wang, E. E. Mendez, Y. Iye, B. Lee, M. H. Kim, and G. E. Stillman, J. Appl. Phys. **60**, 1834 (1986).

[5]W. I. Wang, R. F. Marks, and L. Viña, J. Appl. Phys. **59**, 937 (1986).

[6]T. Fukunaga, T. Takamori, and H. Nakashima, J. Cryst. Growth **81**, 85 (1987).

[7]Y. El Khalifi, P. Lefebvre, J. Allègre, B. Gil, H. Mathieu, and T. Fukunaga, Solid State Commun. **75**, 677 (1990).

[8]B. Gil, Y. El Khalifi, H. Mathieu, C. de Paris, J. Massies, G. Neu, T. Fukunaga, and H. Nakashima, Phys. Rev. B **41**, 2885 (1990).

[9]R. Nötzel, N. N. Ledentsov, L. Däweritz, and K. Ploog, Phys. Rev. B **45**, 3507 (1992).

[10]E. Towe, C. G. Fonstad, H. Q. Le, and J. V. Hryniewicz, J. Vac. Sci. Technol. B **7**, 395 (1989).

[11]S. Minagawa and M. Kondow, Electron. Lett. **25**, 413 (1989); S. Minagawa, M. Kondow, and H. Kakibayashi, *ibid.* **25**, 1439 (1989).

[12]P. N. Uppal, J. S. Ahearn, and D. P. Musser, J. Appl. Phys. **62**, 3766 (1987).

[13]Z. V. Popovic, M. Cardona, E. Richter, D. Strauch, L. Tapfer, and K. Ploog, Phys. Rev. B **40**, 1207 (1989).

[14]L. W. Molenkamp, G. E. W. Bauer, R. Eppenga, and C. T. Foxon, Phys. Rev. B **38**, 6147 (1988).

[15]E. M. Clausen, E. Kapon, M. C. Tamargo, and D. M. Hwang, Appl. Phys. Lett. **56**, 776 (1990).

[16]Y. Moroshita, Y. Nomura, S. Goto, Y. Katayama, and T. Isu, Surf. Sci. **267**, 17 (1992).

[17]S. Shimomura, S. Ohkubo, Y. Yuba, S. Namba, and S. Hiyamizu, Surf. Sci. **267**, 13 (1992).

[18]C. P. Kuo, S. K. Vong, R. M. Cohen, and G. B. Stringfellow, J. Appl. Phys. **57**, 5428 (1985).

[19]J. M. Hinckley and J. Smith, Phys. Rev. B **42**, 3546 (1990); Appl. Phys. Lett. **60**, 2694 (1991).

[20]C. Mailhiot and D. L. Smith, Phys. Rev. B **35**, 1242 (1987); Rev. Mod. Phys. **62**, 173 (1990), and references therein.

[21]See, for instance, A. Segmüller, I. C. Noyan, and V. S. Speriosu, Prog. Cryst. Growth Charact. **18**, 21 (1989), and references therein.

[22]J. Hornstra and W. J. Bartels, J. Cryst. Growth **44**, 513 (1978).

[23]E. Anastassakis, J. Appl. Phys. **68**, 4561 (1990).

[24]E. A. Caridi and J. B. Stark, Appl. Phys. Lett. **60**, 1441 (1992).

[25]J. H. van der Merwe and E. Bauer, Phys. Rev. B **39**, 3632 (1989).

[26]C. W. Snyder, J. F. Mansfield, and B. G. Orr, Phys. Rev. B **46**, 9551

[27]Y. P. Khapachev and F. N. Chukhovskii, Kristallografiya **34**, 776 (1989) [Sov. Phys. Crystallogr. **34**, 465 (1989)].

[28]O. Brandt, K. Ploog, R. Bierwolf, and M. Hohenstein, Phys. Rev. Lett. **68**, 1339 (1992). (1992).

[29]J. F. Nye, *Physical Properties of Crystals* (Oxford University Press, London, 1964), pp. 93–109 and 131–149.

[30]Y. Nakamura, N. Otsuka, M. D. Lange, R. Sporken, and J. P. Faurie, Appl. Phys. Lett. **60**, 1373 (1992).